HHS Public Access

Author manuscript

Exp Gerontol. Author manuscript; available in PMC 2024 September 01.

Published in final edited form as:

Exp Gerontol. 2024 September ; 194: 112483. doi:10.1016/j.exger.2024.112483.

Autophagy markers LC3 and p62 in aging lumbar motor neurons

Sepideh Jahanian[a], **Miguel Pareja-Cajiao**[a], **Heather M. Gransee**[a], **Gary C. Sieck**[a,b], **Carlos B. Mantilla**[a,b,*]

[a]Department of Anesthesiology & Perioperative Medicine, Mayo Clinic, 200 First Street SW, Rochester, MN 55905, USA

[b]Department of Physiology & Biomedical Engineering, Mayo Clinic, 200 First Street SW, Rochester, MN 55905, USA

Abstract

Autophagy is a ubiquitous process through which damaged cytoplasmic structures are recycled and degraded within cells. Aging can affect autophagy regulation in different steps leading to the accumulation of damaged organelles and proteins, which can contribute to cell dysfunction and death. Motor neuron (MN) loss and sarcopenia are prominent features of neuromuscular aging. Previous studies on phrenic MNs showed increased levels of the autophagy proteins LC3 and p62 in 24 month compared to 6 month old mice, consistent with the onset of diaphragm muscle sarcopenia. In the present study, we hypothesized that aging leads to increased expression of the autophagy markers LC3 and p62 in single lumbar MNs. Expression of LC3 and p62 in lumbar MNs (spinal levels L1–L6) was assessed using immunofluorescence and confocal imaging of male and female mice at 6, 18 and 24 months of age, reflecting 100 %, 90 % and 75 % survival, respectively. A mixed linear model with animal as a random effect was used to compare relative LC3 and p62 expression in choline acetyl transferase-positive MNs across age groups. Expression of LC3 and p62 decreased in the white matter of the lumbar spinal cord with aging, with ~29 % decrease in LC3 and ~ 7 % decrease in p62 expression at 24 months of age compared to 6 months of age. There was no change in LC3 or p62 expression in the gray matter with age. LC3 expression in MNs relative to white matter increased significantly with age, with 150 % increase at 24 months of age compared to 6 months of age. Similarly, p62 expression in MNs relative to white matter increased significantly with age, with ~14 % increase at 24 months of age compared to 6 months of age. No effect of sex or MN pool was observed in LC3 and p62 expression in MNs. Overall, these data suggest autophagy impairment during elongation (increased LC3) and degradation (increased p62) phases with aging in lumbar MNs.

*Corresponding author at: 200 First Street SW, Mary Brigh 2-758, Rochester, MN 55905, USA. mantilla.carlos@mayo.edu (C.B. Mantilla).

CRediT authorship contribution statement

Sepideh Jahanian: Writing – review & editing, Writing – original draft, Visualization, Investigation, Formal analysis, Data curation, Conceptualization. **Miguel Pareja-Cajiao:** Writing – review & editing, Visualization, Validation, Methodology, Investigation, Formal analysis, Data curation. **Heather M. Gransee:** Writing – review & editing, Visualization, Validation, Methodology, Formal analysis. **Gary C. Sieck:** Writing – review & editing, Supervision, Resources, Project administration, Funding acquisition, Conceptualization. **Carlos B. Mantilla:** Writing – review & editing, Visualization, Supervision, Resources, Project administration, Methodology, Funding acquisition, Formal analysis, Data curation, Conceptualization.

Keywords

Autophagy; Aging; Motor neuron; Spinal cord; Neuromuscular dysfunction

1. Introduction

Aging leads to progressive loss of function and susceptibility to disease and death through time-related changes (Harman, 1981). Motor neuron (MN) loss and sarcopenia are characteristics of aging skeletal muscle (Faulkner et al., 2007; Hepple, 2003). There is evidence that the nervous system is a key contributor to both loss of function and mass in aging skeletal muscle (Clark, 2019). Aging-related neuromuscular changes in the lumbar motor system include decreased number of MNs in the spinal cord (Tomlinson and Irving, 1977), loss of peripheral MNs (Hashizume and Kanda, 1995), neuromuscular junction morphology changes and degeneration (Gutmann et al., 1966; Oda, 1984) and the presence of denervation markers such as neuronal cell adhesion molecule (Urbanchek et al., 2001) and specific sodium channel ($Na_V1.5$) antibody (Wang et al., 2005) in some aging muscle fibers.

Studies in various organisms have demonstrated the important role of autophagy in neurodegenerative conditions (Castillo et al., 2013; Lipinski et al., 2010; Ruegsegger and Saxena, 2016) and aging (Carnio et al., 2014; Wohlgemuth et al., 2010). Autophagy is a highly-regulated, multi-phase, ubiquitous process (Fig. 1) through which damaged cytoplasmic structures are recycled and degraded within the cell (Gonzalez Porras et al., 2018; Yang and Klionsky, 2010). It is possible that autophagy impairment can subsequently cause damage to the cell and the age-related neuromuscular changes we and others have observed, such as motor neuron loss (Fogarty et al., 2018), muscle fiber denervation (Greising et al., 2015) and sarcopenia (Greising et al., 2013).

There is a paucity of data on aging-related autophagy impairment in hindlimb MNs. Understanding the regulatory mechanisms of autophagy and its role in aging can help alleviate the age-related neuromuscular dysfunction comorbidities or can be a target for developing therapeutic agents in the future. We hypothesized that aging leads to increased expression of the autophagy markers LC3 and p62 in single lumbar MNs. Our study focused on LC3 and p62 proteins, as a previous study from our group observed changes in these markers in aging phrenic MNs, while no such changes were found in other autophagy markers like Beclin-1 or ATG complexes (Pareja-Cajiao et al., 2021). The changes observed in these autophagy markers in aging phrenic MNs were consistent with onset of diaphragm muscle sarcopenia found in other studies (Greising et al., 2013). The current study aimed to assess changes in the expression of the autophagy markers LC3 and p62 with aging in lumbar MNs of mice (spinal levels L1–L6), using immunofluorescence imaging.

2. Methods

2.1. Animals

A total number of 18 male and female C57BL/6 mice at 6, 18 and 24 months of age (mo) reflecting 100 %, 90 % and 75 % survival, respectively, were included in this study (3 males and 3 females at each age). Mice were maintained at the Mayo Clinic with a 12-h light cycle with free access to food and water, and group caged by sex and age. All protocols were approved by the Institutional Animal Care and Use Committee and were in compliance with the National Institutes of Health guidelines. At the terminal experiment, mice were anesthetized with intraperitoneal fentanyl (0.3 mg/kg), diazepam (5 mg/kg) and droperidol (15 mg/kg) and euthanized by exsanguination. To validate the method of correlating LC3 and p62 expression in single motor neurons, a separate group of animals (6 mo male, $n = 5$) were treated with either chloroquine (50 mg/kg of intraperitoneal injection, $n = 3$) or saline (vehicle, $n = 2$) for four hours prior to the terminal procedure (Saldarriaga et al., 2023).

2.2. Immunofluorescence

The procedure for immunofluorescence analyses of LC3 and p62 is as previously described (Pareja-Cajiao et al., 2021). Briefly, animals were treated with 4 % paraformaldehyde in 0.1 M phosphate-buffered solution (pH 7.4) by transcardiac perfusion. The lumbar spinal cord was resected from L1 to L6, kept in 4 % paraformaldehyde overnight and then transferred to 30 % sucrose in 0.1 M phosphate-buffered solution (pH 7.4) at 4 °C. The whole resected spinal cords were sectioned transversely at 20 μm thickness and thaw mounted onto Superfrost™ Plus slides (Fisher Scientific, Pittsburgh, PA). Animals were grouped in 3 different batches such that each batch included one animal from each age and sex group. A stereological approach was used to generate equally spaced sets that represent the entirety of the lumbar spinal cord. Sections of the animals from the same batch were mounted on a single set of slides. Each slide was systematically set up to contain up to 7 sections separated by 200 μm per animal. Slides were labeled and kept at −80 °C until further processing.

A single set of 5 slides per animal was selected randomly for immunofluorescence staining and subsequent imaging. Accordingly, ~30–40 sections were stained per animal in a stereological manner. All slides for animals in the same batch were processed at the same time, as in a previous study (Pareja-Cajiao et al., 2021). Briefly, to remove the excess OCT compound, sections were washed in Tris-buffered saline (TBS) followed by 10 mM trisodium citrate containing 0.05 % Tween 20 (pH 6.0) at 80 °C for antigen retrieval. Sections were blocked in 10 % donkey serum in 0.3 % Triton-TBS and then incubated at 4 °C with primary antibodies (5 % donkey serum in 0.3 % Triton-TBS) for LC3 (NB100–2220, rabbit; 1:200; Novus, Centennial, CO), p62 (GPg2-C, guinea pig; 1:100; Progen, Wayne, PA) and choline acetyl transferase (AB144P, goat; 1:1000; Millipore, Burlington, MA). For secondary antibody treatment, sections were washed and incubated at room temperature with Alexa Fluor-conjugated secondary antibodies in 0.3 % Triton-TBS (Alexa Fluor 647 donkey-anti-rabbit [711-605-152], Alexa Fluor 594 donkey-anti-guinea pig [706-585-148], and Alexa Fluor 488 donkey-anti-goat [705-545-147], all 1:200; Jackson Immuno, West Grove, PA). Subsequently, sections were mounted in ProLong™ Gold

Antifade Reagent with DAPI (Thermo Fisher, Waltham, MA), cover-slipped and allowed to cure before imaging.

2.3. Confocal microscopy

An Olympus FluoView FV1200 laser scanning confocal system (Olympus America Inc., Melville, NY) with 4 diode lasers (405, 488, 559 and 635 nm) and 4 fluorescence detectors on an Olympus BX62 microscope was used for immunofluorescence imaging. Gray matter (GM) anatomy was assessed using a panoramic 10× objective (NA 0.3) in order to determine the spinal cord segment level using a standard atlas (Fig. 2A) (Sengul et al., 2012). No further analysis was conducted on this data. Subsequently, image stacks were obtained from choline acetyl transferase (ChAT) positive MNs (Fig. 2B–C) on both sides of the ventral horn from L1-L6 using 20× oil immersion objective (NA 0.8) and 2 μm step size for fluorescence intensity analysis. All images for a single slide were taken using the same laser intensity and detector (voltage, gain, offset) settings, and imaging parameters were verified within a batch and across sessions to achieve equivalent imaging results for the 6-month old sections in each slide.

2.4. Image analysis

Images were processed with MetaMorph (Molecular Devices, San Jose, CA) and NIS-Elements (Nikon, Melville, NY). A maximum intensity projection image was obtained for each section. Three regions of interest (ROI) of constant shape/size were drawn for both GM and WM. MNs were identified as ChAT-positive cells of area > 200 μm^2, and ROIs were manually drawn around mid-nuclear MNs (Fig. 2D). MN ROI area was used as an estimate of MN somal surface area.

Mean LC3 and p62 fluorescence intensities were subsequently analyzed in separate channels for the marked ROIs. Each MN ROI was assigned a spinal cord level and MN pool by comparing the section and the MN location to a standard mouse spinal cord atlas (Sengul et al., 2012). The average of three ROIs for WM and GM was calculated for each image separately. Average WM intensity was subtracted from raw measurements of MN LC3 and p62 intensity and presented as a ratio to average WM intensity. Because subsequent analyses showed a change in WM fluorescence intensity with age, we also presented the data as a ratio to GM (raw LC3 and p62 values subtracted by average GM per image divided by average GM). Intensity of LC3 and p62 of the WM, GM and MN (both compared to WM and GM) were normalized to the 6 mo female (present on all slides) on each slide to omit the slide effect. The normalized intensities were used for comparison across age groups. Starting from this point in the text, the terms “relative LC3” and “relative p62” refer to values adjusted for WM and normalized to the 6 mo female section on each slide, unless explicitly stated otherwise.

2.5. Statistical analyses

LC3 and p62 intensities were compared across different age groups using a mixed linear model. The model included age, sex, and their interactions as fixed effects and animal was treated as random effect. Tukey-Kramer HSD test was used where post hoc analyses were needed. *P*-values < 0.05 were considered statistically significant. Data are presented as mean

with 95 % confidence interval (CI), in arbitrary units (au) and compared to the 6 mo female group unless otherwise specified. MN soma size tertiles were stratified into 3 groups based on the boundaries of soma size tertiles in the 6 mo group (i.e., smaller MNs in the lower tertile, and larger MNs in the upper tertile), similar to previous studies (Fogarty, 2023; Fogarty et al., 2018). In each tertile and age group, the distribution of MNs were reported as N (%) and the ROI area of MN soma was reported as mean ± SD (μm^2, with 95 % CI). The relationship between two ordinal variables was determined by Chi-square test. The effect size was calculated by square root of the average Pearson Chi-square. JMP 14.1.0 (SAS Institute Inc., Cary, NY) was used to analyze the data.

3. Results

A total of 18 mice (9 males, 9 females) across three age groups (6, 18 and 24 mo; $n = 3$ per sex and age groups) were used for the experiment. MNs in the lumbar enlargement were identified in spinal cord cross-sections by ChAT immunofluorescence (~3–5/side). Spinal cord sections were included in a systematic, random manner such that for each animal ~30–40 sections were assessed for ChAT-positive MNs containing the nucleus and at least 200 μm^2 in cross-sectional area. In total, the relative fluorescence intensity of LC3 and p62 was measured in 1298 ChAT-positive MNs meeting these inclusion criteria in 6, 18, and 24 mo mice (372, 545 and 381 MNs per age group, respectively). Based on the shape of the spinal cord ventral horn, distribution of ChAT-positive cells and the relationship to neighboring sections, the spinal cord level was determined for each section. Across all groups, most of the MNs studied were located at L3 (33%, 38 % and 47 % of the 6, 18 and 24 mo groups, respectively; Table 1) and in areas consistent with the location of quadriceps MNs (Table 2). MNs located in regions corresponding to crural MNs (crural flexors and extensors including soleus, gastrocnemius, extensor digitorum longus, and tibialis anterior muscles) were 17 % of the total MNs (23 %, 17 %, 10 % of the total MNs in 6, 18 and 24 mo groups, respectively; Table 2). A small proportion of MNs were located in regions corresponding to axial and quadratus lumborum muscles (12 % and 8 % of total MNs, respectively).

3.1. LC3 expression increases in lumbar motor neurons with aging

The mixed linear model showed a significant effect on LC3 expression in WM of age ($F_{2,8} = 49$, $P < 0.0001$), sex ($F_{1,18} = 51$, $P < 0.0001$), and their interaction ($F_{2,8} = 23$, $P < 0.001$). Overall, LC3 expression in WM significantly decreased by 17 % and 29 % in 18 and 24 mo mice, respectively, compared to 6 mo mice (Fig. 3). LC3 expression in the WM in male mice was greater than in females, and post-hoc analyses revealed that this sex difference was only evident in 6 mo mice, with males having 45 % higher LC3 expression in WM than females ($P < 0.05$). LC3 expression in GM was not significantly affected by age ($F_{2,10} < 1$, $P > 0.05$) or sex ($F_{1,15} = 4$, $P > 0.05$).

There was an effect on relative LC3 expression in MNs of age ($F_{2,15} = 14$, $P < 0.001$) but not of sex ($F_{1,13} < 1$, $P > 0.05$) or their interaction ($F_{2,12} < 1$, $P > 0.05$). Overall, relative LC3 expression in MNs did not change at 18 mo compared to 6 mo. At 24 mo, relative LC3 expression in MNs was significantly increased by 150 % compared to 6 mo and by 60 %

compared to 18 mo groups. There was no effect on LC3 expression in MNs relative to GM of age ($F_{2,13} = 0$, $P > 0.05$) or sex ($F_{1,11} < 1$, $P > 0.05$).

3.2. p62 expression increases in lumbar motor neurons with aging

The mixed linear model showed a significant effect on p62 expression in WM of age ($F_{2,13} = 10$, $P < 0.01$), sex ($F_{1,17} = 7$, $P = 0.01$) and their interaction ($F_{2,12} = 4$, $P = 0.04$). Overall, p62 expression in the WM significantly decreased by 7 % in 18 and 24 mo mice compared to 6 mo mice (Fig. 4). Across all age groups, male mice demonstrated ~1 % higher p62 expression in WM than female mice. Post-hoc analyses showed that 6 mo males expressed 13 % higher p62 expression in WM compared to 18 and 24 mo male and female mice ($P < 0.05$). There was no effect of age ($F_{2,13} = 1$, $P > 0.05$) or sex ($F_{1,15} = 1$, $P > 0.05$) on p62 expression in the GM.

There was a significant effect on relative p62 expression in MNs of age ($F_{2,16} = 4$, $P = 0.04$) but not of sex ($F_{1,14} < 1$, $P > 0.05$) or their interaction ($F_{2,13} = 1$, $P > 0.05$). Post-hoc analyses showed that relative p62 expression in MNs was unchanged at 18 mo and then increased significantly by ~14 % in 24 mo mice compared to 6 mo mice ($P < 0.05$). The p62 expression in MNs relative to GM was not significantly changed with age ($F_{2,16} < 1$, $P > 0.05$) or sex ($F_{1,14} = 1$, $P > 0.05$).

3.3. Changes in LC3 and p62 at motor neurons pools

We also examined the changes in relative LC3 and p62 expression in MNs in specific MN pools (quadriceps, axial/quadratus lumborum, crural extensors, crural flexors, and hamstrings). Our results did not reveal any effects of MN pool on relative LC3 or p62 expression in the MNs ($F_{4,357} < 1$, $P > 0.05$ for relative LC3 and $F_{4,248} = 1$, $P > 0.05$ for relative p62). Relative expression of LC3 and p62 in the MN pools of largest proportion are as follows. In quadriceps MN pool, relative LC3 in MNs at 24 mo was 99 % higher than 6 mo and 64 % higher than 18 mo mice. Additionally, relative p62 in quadriceps MNs was 14 % greater at 24 mo compared to 6 mo. In hamstrings muscles, relative LC3 expression was increased ~330 % at 24 mo compared to 6 mo and 81 % compared to 18 mo. The relative p62 expression was increased by 6 % at 24 mo compared to 6 mo.

3.4. Changes in MN soma size with age

MN somal surface area of ChAT-positive MNs meeting inclusion criteria was estimated from the manually-drawn ROI area and grouped into tertiles according to size (somal surface area) based on the 6 mo group. The mean MN somal size in smaller, middle and larger tertiles were 385 ± 94, 666 ± 88, and 1065 ± 184 μm^2, respectively (Fig. 5). In 18 mo mice, 211 MNs (39 %) were in the smaller, 172 MNs (32 %) in the middle and 162 MNs (30 %) were in the larger tertile. In the 24 mo group, 196 (52 %), 118 (31 %), and 67 (18 %) MNs were in the smaller, middle and larger tertiles, respectively. There was a significant relationship between age and MN somal size tertile (X^2 [4, $N = 1298$] = 36, $P < 0.0001$) with effect size of 0.2. There was no effect of MN somal size on relative LC3 or relative p62 in MNs ($F_{2,1284} < 1$, $P > 0.05$).

When looking at individual MN pools, there was a significant relationship between age and MN somal size tertile in both crural and quadriceps MN pools ($P < 0.05$). In axial and quadratus lumborum MN pools there was not a significant association between age and MN somal size tertile ($P > 0.05$). In hamstring MN pool, frequency of MNs in smaller tertile increased with age (28 %, 31 % and 58 % of the total MNs at 6, 18, and 24 mo, respectively). MNs in the larger tertile comprised 31 % of the MNs at 6 mo which increased to 40 % at 18 mo and subsequently decreased to 29 % at 24 mo.

3.5. Correlation between aging-related changes in LC3 and p62 at individual motor neurons

A visual correlation between relative LC3 and p62 fluorescence intensity in individual MNs was analyzed in MN somal size tertile groups (Fig. 6). This correlation was validated with lysosomal inhibitor chloroquine treatment in a subset of animals (6 mo), which did not show any difference in LC3 or p62 expression in single MNs in chloroquine treated animals compared to that of vehicle treated animals. Across all tertiles, there was an upward shift with aging, reflecting the age-related increase in relative LC3 expression (autophagy impairment). Additionally, across all tertiles there was a leftward shift of the ellipses with aging, reflecting an increase in relative p62 expression (autophagy impairment). Overall, there is a shift towards increased relative LC3 expression that progresses at both 18 and 24 mo, and increased relative p62 expression at 18 mo. This pattern is consistent across all MN somal size tertiles.

4. Discussion

Aging consists of a series of physiological changes that ultimately result in reduced ability to respond to stress and maintain biological functions (Harman, 1981; López-Otín et al., 2013). Autophagy is a highly regulated process which is responsible for clearing damaged cytoplasmic structures and altered proteins (Klionsky et al., 2021; Ravikumar et al., 2005). Therefore, impaired autophagy results in accumulation of these components as well as markers that reflect each phase of the autophagy process (Kohli and Roth, 2010). Autophagy is composed of a series of dynamic phases with key molecular targets to exploit as autophagy markers. Beclin-1 is involved in the induction phase (Kang et al., 2011); ATG3, ATG7, and ATG5/12/16 are involved in the elongation phase; and LC3 lipidation (Hanada et al., 2007; Martinet et al., 2013; Mizushima, 2020), p62 (Bjørkøy et al., 2009) and lysosomal markers (LAMP1 and LAMP2) (Yoshii and Mizushima, 2017) are involved in the degradation phase. LC3 and p62 proteins are selectively degraded by autophagy and are commonly used to evaluate autophagy impairment (Komatsu et al., 2010).

Our previous study in phrenic MNs found no change in Beclin-1, ATG7 or ATG5/12 expression with age, suggesting minimal effects of aging on the initiation phases of autophagy in cervical MNs (Pareja-Cajiao et al., 2021). However, expression of LC3 and p62 in phrenic MNs were significantly increased by 24 mo, indicating autophagosome accumulation and impaired autophagy in cervical MNs (Pareja-Cajiao et al., 2021). The present study showed significant changes in the relative expression of the autophagy markers LC3 and p62 in lumbar MNs between 6, 18 and 24 mo mice. MN relative LC3 expression

increased with age; compared to 6 mo mice, relative LC3 expression increased ~150 % in the 24 mo mice, consistent with impaired elongation of autophagy. MN relative p62 expression increased ~15 % in the MNs of 24 mo mice compared to the 6 mo mice. Expression of LC3 and p62 in the lumbar MNs did not change with age relative to the GM, suggesting the extent of the impaired autophagy was not limited to MN somata but included neuropil and glial cells.

While there are inherent limitations of immunohistochemistry methods for quantifying protein expression, our approach offers several strengths that warrant confidence in our interpretations of autophagy marker expression. Firstly, multiple steps were used to provide a comprehensive assessment of protein expression across all ages and sex in each slide, allowing for robust comparisons within and between slides, batches, and imaging sessions; thus, minimizing potential confounding factors and enhancing the reliability of our findings. Additionally, our approach allows us to focus on examining protein expression in single motor neurons, which adds specificity to our analysis. Other techniques to measure protein expression (e.g., immunoblotting in whole tissue homogenates) do not provide the specificity to determine age-related changes in the expression of autophagy markers at single MNs.

Autophagy has been shown to play an important role in protein regulation in neurodegenerative diseases. A study of L1–L5 lumbar spinal cord of postmortem patients with amyotrophic lateral sclerosis (ALS) showed autophagosomes and autolysosomes in the cytoplasm of both normal-appearing and degenerated MNs in all ALS patients analyzed, a feature of upregulated autophagy (Sasaki, 2011). In an ALS mouse model, LC3 protein expression was significantly increased in spinal cord in symptomatic stage Tg G93A-SOD1 mice (Crippa et al., 2013). Increased expression of autophagy markers is evident in other neurodegenerative diseases, such as increased LC3 and p62 in the hippocampus of a mouse model of Alzheimer’s disease (Jiang et al., 2022) and increased p62 in dopaminergic neurons of a mouse model of Parkinson’s disease (Song et al., 2016). There is scarce evidence on autophagy markers in aging spinal cord; however, in aging neurons of mouse hypothalamus, p62 accumulation was observed reflecting impaired autophagy (Kaushik et al., 2012). Overall, these findings in aging and neurodegenerative diseases are in line with our study and suggest that the increase of autophagy markers reflect neurodegeneration caused by impaired autophagy in old age.

Evidence of autophagy impairment is present in glial cells in aging models and models of neurodegeneration. Increased LC3 and p62 expression in astrocytes is evident in the hippocampus of neurodegenerative diseases, including mouse models of Alzheimer’s disease (Gong et al., 2023), as well as after spinal cord injury (Muñoz-Galdeano et al., 2018). Overall, this is in line with our findings, suggesting that the changes in autophagy with aging are not limited to MNs, as astrocytes have been shown to express both LC3 and p62 in old age (Wang and Xu, 2020). Autophagy marker expression in WM in our study did not increase with age. There is a paucity in literature involving autophagy in aging axons or oligodendrocytes. In an ALS mouse model, LC3 and p62 aggregates were evident in neurofilament-positive axons (Liang et al., 2019). Markers of autophagy impairment are also evident after CNS damage in traumatic brain (Sarkar et al., 2014) and after spinal cord

injury (Liu et al., 2015; Muñoz-Galdeano et al., 2018). Increased relative autophagy markers with age in the current study are consistent with a greater extent of autophagy changes in the MNs than in the WM (oligodendrocytes and axons).

A feature of aging in the neuromuscular system is the loss of MNs. There is evidence that impaired autophagy in old age contributes to neurodegeneration and increases the vulnerability of aging MNs (Kenyon, 2010; Leidal et al., 2018; Nixon, 2013). Previous studies have shown age-related MN loss in anterior horn of the lumbar spinal cord of mice (Caccia et al., 1979; Piekarz et al., 2020), rats (Edstrom and Larsson, 1987; Hashizume et al., 1988; Jacob, 1998), and humans (Tomlinson and Irving, 1977). In mice, there was a ~17 % loss of lumbar MNs at 16–18 mo and ~41 % loss by 24–28 mo compared to 2–6 mo mice (Piekarz et al., 2020). In post-mortem human lumbar and sacral spinal cord there was ~36 % decrease in total MNs of 81–95 year old cases compared to 13–40 year old cases (Tomlinson and Irving, 1977). There is growing evidence of differences in sarcopenia across muscle groups with type II muscle fibers and larger MNs being more affected by aging (Ciciliot et al., 2013; Fogarty et al., 2018; Hou et al., 2019). Loss of phrenic MNs was recently reported in old rats (24 mo compared to 6 mo) with selective loss of larger MNs consistent with atrophy of type II muscle fibers and denervation in old age (Fogarty et al., 2018). Larger MNs are mainly responsible for innervating fast-twitch (type II) muscle fibers (Burke et al., 1973; Henneman, 1957). In the present study, most lumbar MNs studied innervated the quadriceps muscle (47 %) which primarily consists of type II muscle fibers. A study of plantaris muscle showed that the cross-sectional area of type II muscle fibers in 30 mo rats was 37 % less compared to 9 mo rats (Holloszy et al., 1991). In rat hindlimb (tibialis anterior and soleus muscles) decreased proportion of type II fibers was observed at 16 and 34 mo compared to 3 mo which was accompanied by decreased number of larger MNs innervating these muscles (Ishihara et al., 1987). In general agreement, in the present study there were fewer larger MNs in the lumbar spinal cord of 24 mo mice compared to 6 mo mice. Of note, our results are limited to 2D cross-sectional area where cells are cut in horizontal fashion and does not account for MN somal volume in vertical planes.

We did not observe any sex-related changes in relative LC3 and p62 expression in lumbar MNs, but there were differences in WM LC3 expression in 6 mo mice. Similarly, functional studies of aging mouse diaphragm muscle force performance (Greising et al., 2015) and rat phrenic MN loss (Fogarty et al., 2018) did not demonstrate sexual differences, consistent with minimal effects of sex on aging. Our previous study in cervical MNs (Pareja-Cajiao et al., 2021) showed higher p62 expression in 6 mo females compared to male mice, with no difference in relative p62 expression across age groups consistent with experimental data supporting sexual differences in autophagy at young age (Lista et al., 2011; Yang and Klionsky, 2009) which could be due to the neuroprotective effect of sex hormones (Brann et al., 2007; Xiang et al., 2019).

5. Conclusion

Taken together, our results showed increased accumulation of autophagy markers LC3 (reflecting autophagy elongation phase) and p62 (reflecting autophagosome degradation) in the lumbar MNs of aging mice and are consistent with autophagosome accumulation in old

age. These results were observed across different MN pools in the lumbar spinal cord and were consistent with our previous study in cervical MNs. We also found a decrease in larger MNs in older mice. Whether there is a link between impaired autophagy in larger cells which leads to their apoptosis and death needs to be further investigated. Indeed, subsequent studies are needed to elucidate the mechanism behind the MN size-dependent changes in aging.

Declaration of competing interest

This work was funded by NIH grant R01 AG057052 and the Mayo Clinic.

References

Bjørkøy G, Lamark T, Pankiv S, Øvervatn A, Brech A, Johansen T, 2009. Monitoring autophagic degradation of p62/SQSTM1. Methods Enzymol. 452, 181–197. [PubMed: 19200883]

Brann DW, Dhandapani K, Wakade C, Mahesh VB, Khan MM, 2007. Neurotrophic and neuroprotective actions of estrogen: basic mechanisms and clinical implications. Steroids 72, 381–405. [PubMed: 17379265]

Burke RE, Levine DN, Tsairis P, Zajac III FE, 1973. Physiological types and histochemical profiles in motor units of the cat gastrocnemius. J. Physiol 234, 723–748. [PubMed: 4148752]

Caccia MR, Harris JB, Johnson MA, 1979. Morphology and physiology of skeletal muscle in aging rodents. Muscle Nerve 2, 202–212. [PubMed: 159414]

Carnio S, LoVerso F, Baraibar MA, Longa E, Khan MM, Maffei M, Sandri M, 2014. Autophagy impairment in muscle induces neuromuscular junction degeneration and precocious aging. Cell Rep. 8, 1509–1521. [PubMed: 25176656]

Castillo K, Valenzuela V, Matus S, Nassif M, Onate M, Fuentealba Y, Hetz C, 2013. Measurement of autophagy flux in the nervous system in vivo. Cell Death Dis. 4, e917. [PubMed: 24232093]

Ciciliot S, Rossi AC, Dyar KA, Blaauw B, Schiaffino S, 2013. Muscle type and fiber type specificity in muscle wasting. Int. J. Biochem. Cell Biol 45, 2191–2199. [PubMed: 23702032]

Clark BC, 2019. Neuromuscular changes with aging and sarcopenia. J. Frailty Aging 8, 7–9. [PubMed: 30734824]

Crippa V, Boncoraglio A, Galbiati M, Aggarwal T, Rusmini P, Giorgetti E, Poletti A, 2013. Differential autophagy power in the spinal cord and muscle of transgenic ALS mice. Front. Cell. Neurosci 7, 234. [PubMed: 24324403]

Edstrom L, Larsson L, 1987. Effects of age on contractile and enzyme-histochemical properties of fast- and slow-twitch single motor units in the rat. J. Physiol 392, 129–145. [PubMed: 2965761]

Faulkner JA, Larkin LM, Claflin DR, Brooks SV, 2007. Age-related changes in the structure and function of skeletal muscles. Clin. Exp. Pharmacol. Physiol 34, 1091–1096. [PubMed: 17880359]

Fogarty MJ, 2023. Loss of larger hypoglossal motor neurons in aged Fischer 344 rats. Respir. Physiol. Neurobiol 314, 104092. [PubMed: 37331418]

Fogarty MJ, Omar TS, Zhan WZ, Mantilla CB, Sieck GC, 2018. Phrenic motor neuron loss in aged rats. J. Neurophysiol 119, 1852–1862. [PubMed: 29412773]

Gong C, Bonfili L, Zheng Y, Cecarini V, Cuccioloni M, Angeletti M, Eleuteri AM, 2023. Immortalized Alzheimer's disease astrocytes: characterization of their proteolytic systems. Mol. Neurobiol 60, 2787–2800. [PubMed: 36729287]

Gonzalez Porras MA, Sieck GC, Mantilla CB, 2018. Impaired autophagy in motor neurons: a final common mechanism of injury and death. Physiology 33, 211–224. [PubMed: 29638184]

Greising SM, Mantilla CB, Gorman BA, Ermilov LG, Sieck GC, 2013. Diaphragm muscle sarcopenia in aging mice. Exp. Gerontol 48, 881–887. [PubMed: 23792145]

Greising SM, Mantilla CB, Medina-Martinez JS, Stowe JM, Sieck GC, 2015. Functional impact of diaphragm muscle sarcopenia in both male and female mice. Am. J. Physiol. Lung Cell. Mol. Physiol 309, L46–L52. [PubMed: 25934669]

Gutmann E, Hanikova M, Hajek I, Klicpera M, Syrovy I, 1966. The postdenervation hypertrophy of the diaphragm. Physiol. Bohemoslov 15, 508–524. [PubMed: 4225269]

Hanada T, Noda NN, Satomi Y, Ichimura Y, Fujioka Y, Takao T, Ohsumi Y, 2007. The Atg12-Atg5 conjugate has a novel E3-like activity for protein lipidation in autophagy. J. Biol. Chem 282, 37298–37302. [PubMed: 17986448]

Harman D, 1981. The aging process. Proc. Natl. Acad. Sci. U. S. A 78, 7124–7128. [PubMed: 6947277]

Hashizume K, Kanda K, 1995. Differential effects of aging on motoneurons and peripheral nerves innervating the hindlimb and forelimb muscles of rats. Neurosci. Res 22, 189–196. [PubMed: 7566699]

Hashizume K, Kanda K, Burke RE, 1988. Medial gastrocnemius motor nucleus in the rat: age-related changes in the number and size of motoneurons. J. Comp. Neurol 269, 425–430. [PubMed: 3372722]

Henneman E, 1957. Relation between size of neurons and their susceptibility to discharge. Science 126, 1345–1346. [PubMed: 13495469]

Hepple RT, 2003. Sarcopenia–a critical perspective. Sci. Aging Knowl. Environ 2003, pe31.

Holloszy JO, Chen M, Cartee GD, Young JC, 1991. Skeletal muscle atrophy in old rats: differential changes in the three fiber types. Mech. Ageing Dev 60, 199–213. [PubMed: 1745075]

Hou Y, Dan X, Babbar M, Wei Y, Hasselbalch SG, Croteau DL, Bohr VA, 2019. Ageing as a risk factor for neurodegenerative disease. Nat. Rev. Neurol 15, 565–581. [PubMed: 31501588]

Ishihara A, Naitoh H, Katsuta S, 1987. Effects of ageing on the total number of muscle fibers and motoneurons of the tibialis anterior and soleus muscles in the rat. Brain Res. 435, 355–358. [PubMed: 3427464]

Jacob JM, 1998. Lumbar motor neuron size and number is affected by age in male F344 rats. Mech. Ageing Dev 106, 205–216. [PubMed: 9883984]

Jiang R, Shimozawa M, Mayer J, Tambaro S, Kumar R, Abelein A, Nilsson P, 2022. Autophagy impairment in app Knock-in Alzheimer's model mice. Front. Aging Neurosci 14, 878303. [PubMed: 35663567]

Kang R, Zeh HJ, Lotze MT, Tang D, 2011. The Beclin 1 network regulates autophagy and apoptosis. Cell Death Differ. 18, 571–580. [PubMed: 21311563]

Kaushik S, Arias E, Kwon H, Lopez NM, Athonvarangkul D, Sahu S, Singh R, 2012. Loss of autophagy in hypothalamic POMC neurons impairs lipolysis. EMBO Rep. 13, 258–265. [PubMed: 22249165]

Kenyon CJ, 2010. The genetics of ageing. Nature 464, 504–512. [PubMed: 20336132]

Klionsky DJ, Abdel-Aziz AK, Abdelfatah S, Abdellatif M, Abdoli A, Abel S, Tong CK, 2021. Guidelines for the use and interpretation of assays for monitoring autophagy (4th edition). Autophagy 17, 1–382. [PubMed: 33634751]

Kohli L, Roth KA, 2010. Autophagy: cerebral home cooking. Am. J. Pathol 176, 1065–1071. [PubMed: 20150434]

Komatsu M, Kurokawa H, Waguri S, Taguchi K, Kobayashi A, Ichimura Y, Yamamoto M, 2010. The selective autophagy substrate p62 activates the stress responsive transcription factor Nrf2 through inactivation of Keap1. Nat. Cell Biol 12, 213–223. [PubMed: 20173742]

Leidal AM, Levine B, Debnath J, 2018. Autophagy and the cell biology of age-related disease. Nat. Cell Biol 20, 1338–1348. [PubMed: 30482941]

Liang C, Shao Q, Zhang W, Yang M, Chang Q, Chen R, Chen J-F, 2019. Smcr8 deficiency disrupts axonal transport-dependent lysosomal function and promotes axonal swellings and gain of toxicity in C9ALS/FTD mouse models. Hum. Mol. Genet 28, 3940–3953. [PubMed: 31625563]

Lipinski MM, Zheng B, Lu T, Yan Z, Py BF, Ng A, Yuan J, 2010. Genome-wide analysis reveals mechanisms modulating autophagy in normal brain aging and in Alzheimer's disease. Proc. Natl. Acad. Sci. U. S. A 107, 14164–14169. [PubMed: 20660724]

Lista P, Straface E, Brunelleschi S, Franconi F, Malorni W, 2011. On the role of autophagy in human diseases: a gender perspective. J. Cell. Mol. Med 15, 1443–1457. [PubMed: 21362130]

Liu S, Sarkar C, Dinizo M, Faden AI, Koh EY, Lipinski MM, Wu J, 2015. Disrupted autophagy after spinal cord injury is associated with ER stress and neuronal cell death. Cell Death Dis. 6, e1582. [PubMed: 25569099]

López-Otín C, Blasco MA, Partridge L, Serrano M, Kroemer G, 2013. The hallmarks of aging. Cell 153, 1194–1217. [PubMed: 23746838]

Martinet W, Schrijvers DM, Timmermans JP, Bult H, De Meyer GR, 2013. Immunohistochemical analysis of macroautophagy: recommendations and limitations. Autophagy 9, 386–402. [PubMed: 23242143]

Mizushima N, 2020. The ATG conjugation systems in autophagy. Curr. Opin. Cell Biol 63, 1–10. [PubMed: 31901645]

Muñoz-Galdeano T, Reigada D, Del Águila Á, Velez I, Caballero-López MJ, Maza RM, Nieto-Díaz M, 2018. Cell specific changes of autophagy in a mouse model of contusive spinal cord injury. Front. Cell. Neurosci 12, 164. [PubMed: 29946241]

Nixon RA, 2013. The role of autophagy in neurodegenerative disease. Nat. Med 19, 983–997. [PubMed: 23921753]

Oda K, 1984. Age changes of motor innervation and acetylcholine receptor distribution on human skeletal muscle fibres. J. Neurol. Sci 66, 327–338. [PubMed: 6530617]

Pareja-Cajiao M, Gransee HM, Stowe JM, Rana S, Sieck GC, Mantilla CB, 2021. Age-related impairment of autophagy in cervical motor neurons. Exp. Gerontol 144, 111193. [PubMed: 33290859]

Piekarz KM, Bhaskaran S, Sataranatarajan K, Street K, Premkumar P, Saunders D, Van Remmen H, 2020. Molecular changes associated with spinal cord aging. Geroscience 42, 765–784. [PubMed: 32144690]

Ravikumar B, Acevedo-Arozena A, Imarisio S, Berger Z, Vacher C, O'Kane CJ, Rubinsztein DC, 2005. Dynein mutations impair autophagic clearance of aggregate-prone proteins. Nat. Genet 37, 771–776. [PubMed: 15980862]

Ruegsegger C, Saxena S, 2016. Proteostasis impairment in ALS. Brain Res. 1648, 571–579. [PubMed: 27033833]

Saldarriaga CA, Alatout MH, Khurram OU, Gransee HM, Sieck GC, Mantilla CB, 2023. Chloroquine impairs maximal transdiaphragmatic pressure generation in old mice. J. Appl. Physiol 135, 1126–1134. [PubMed: 37823202]

Sarkar C, Zhao Z, Aungst S, Sabirzhanov B, Faden AI, Lipinski MM, 2014. Impaired autophagy flux is associated with neuronal cell death after traumatic brain injury. Autophagy 10, 2208–2222. [PubMed: 25484084]

Sasaki S, 2011. Autophagy in spinal cord motor neurons in sporadic amyotrophic lateral sclerosis. J. Neuropathol. Exp. Neurol 70, 349–359. [PubMed: 21487309]

Sengul G, Watson C, Tanaka I, Paxinos G, 2012. Atlas of the Spinal Cord: Mouse, Rat, Rhesus, Marmoset, and Human. Academic Press.

Song P, Li S, Wu H, Gao R, Rao G, Wang D, Chen Q, 2016. Parkin promotes proteasomal degradation of p62: implication of selective vulnerability of neuronal cells in the pathogenesis of Parkinson's disease. Protein Cell 7, 114–129. [PubMed: 26746706]

Tomlinson BE, Irving D, 1977. The numbers of limb motor neurons in the human lumbosacral cord throughout life. J. Neurol. Sci 34, 213–219. [PubMed: 925710]

Urbanchek MG, Picken EB, Kalliainen LK, Kuzon WM Jr., 2001. Specific force deficit in skeletal muscles of old rats is partially explained by the existence of denervated muscle fibers. J. Gerontol. A Biol. Sci. Med. Sci 56, B191–B197. [PubMed: 11320099]

Wang J-L, Xu C-J, 2020. Astrocytes autophagy in aging and neurodegenerative disorders. Biomed. Pharmacother 122, 109691. [PubMed: 31786465]

Wang ZM, Zheng Z, Messi ML, Delbono O, 2005. Extension and magnitude of denervation in skeletal muscle from ageing mice. J. Physiol 565, 757–764. [PubMed: 15890702]

Wohlgemuth SE, Seo AY, Marzetti E, Lees HA, Leeuwenburgh C, 2010. Skeletal muscle autophagy and apoptosis during aging: effects of calorie restriction and life-long exercise. Exp. Gerontol 45, 138–148. [PubMed: 19903516]

Xiang J, Liu X, Ren J, Chen K, Wang HL, Miao YY, Qi MM, 2019. How does estrogen work on autophagy? Autophagy 15, 197–211. [PubMed: 30208759]

Yang Z, Klionsky DJ, 2009. An overview of the molecular mechanism of autophagy. Curr. Top. Microbiol. Immunol 335, 1–32. [PubMed: 19802558]

Yang Z, Klionsky DJ, 2010. Mammalian autophagy: core molecular machinery and signaling regulation. Curr. Opin. Cell Biol 22, 124–131. [PubMed: 20034776]

Yoshii SR, Mizushima N, 2017. Monitoring and measuring autophagy. Int. J. Mol. Sci 18.

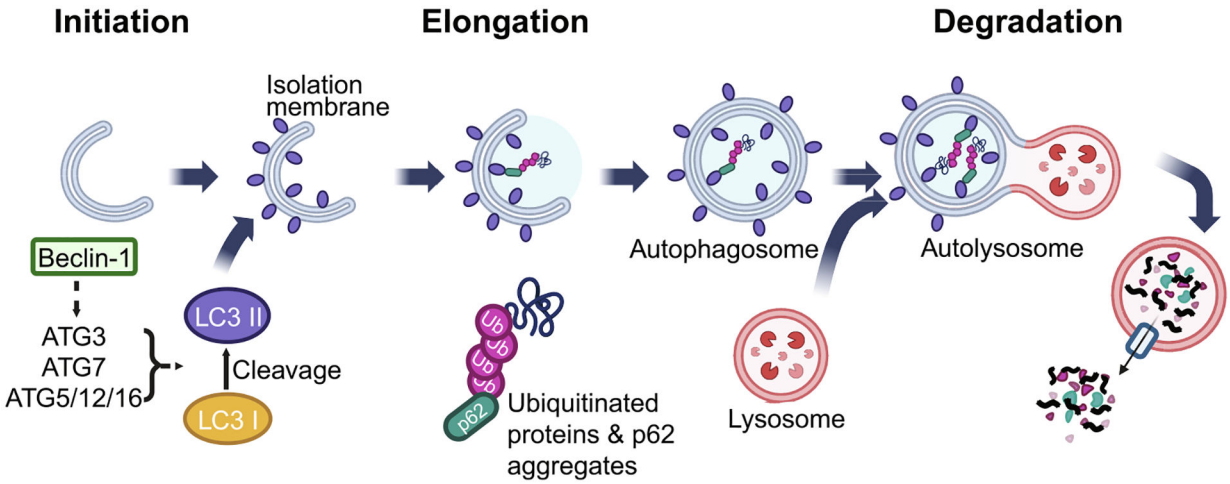

Fig. 1.

Autophagy consists of three main phases. During initiation, damaged organelles trigger activation of Beclin-1. The elongation phase involves conversion of LC3I to LC3II through lipidation with the aid of ATG3, ATG7 and the ATG5/12/16 complex recruitment. Disturbance during the elongation phase can lead to LC3 accumulation. During this phase, p62 binds to both ubiquitinated proteins and LC3 on the autophagosomal membrane, acting as a bridge that facilitates the engulfment of cargo by autophagosomes. Ultimately, after the autophagosome-lysosome fusion, the autophagosome containing the engulfed cargo gets sequestered within the lysosome during the degradation phase. Elevated p62 levels are seen with degradation phase impairment as receptor protein p62 plays an important role in autophagosome formation and its degradation via lysosome. Figure created with Biorender.com.

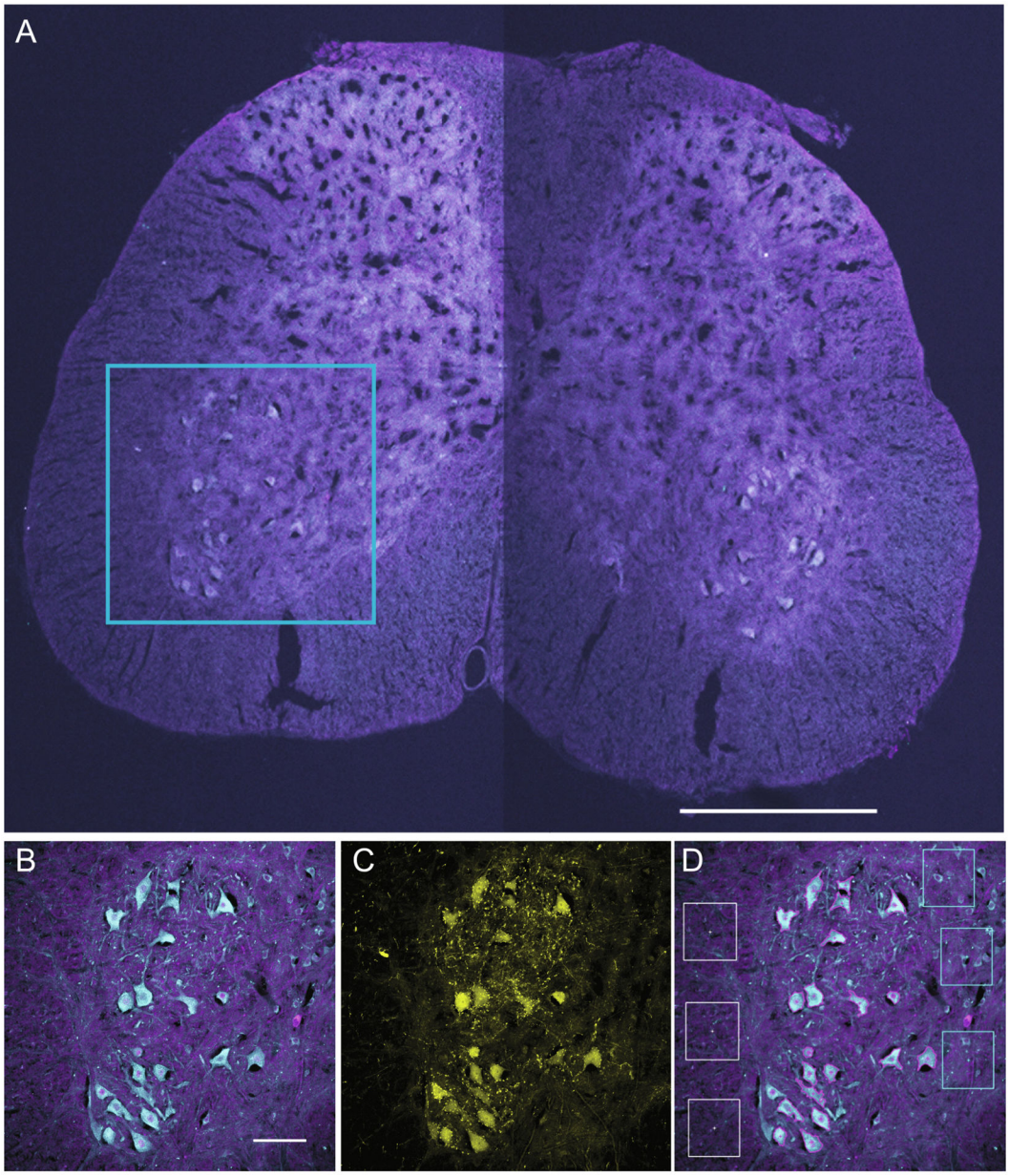

Fig. 2.

Lumbar spinal cord images obtained by confocal microscopy used to measure LC3 and p62 expression in motor neurons. (A) Stitched, multicolor, low magnification image was used to identify the spinal cord segment level by comparing to a mouse standard atlas (Sengul et al., 2012). This section was identified as L5. High magnification images of the ventral horn (inset, box outlined in blue) were used for fluorescence intensity measurements. (B, C) Maximum intensity projection images for LC3 (magenta), p62 (cyan) and motor neurons (ChAT+, yellow) corresponding to the inset in A. (D) Immunofluorescence intensity was measured for both LC3 and p62 in ChAT-positive motor neurons, gray matter (right squares), and white matter (left squares). Bar, 500 μm in A and 100 μm in B.

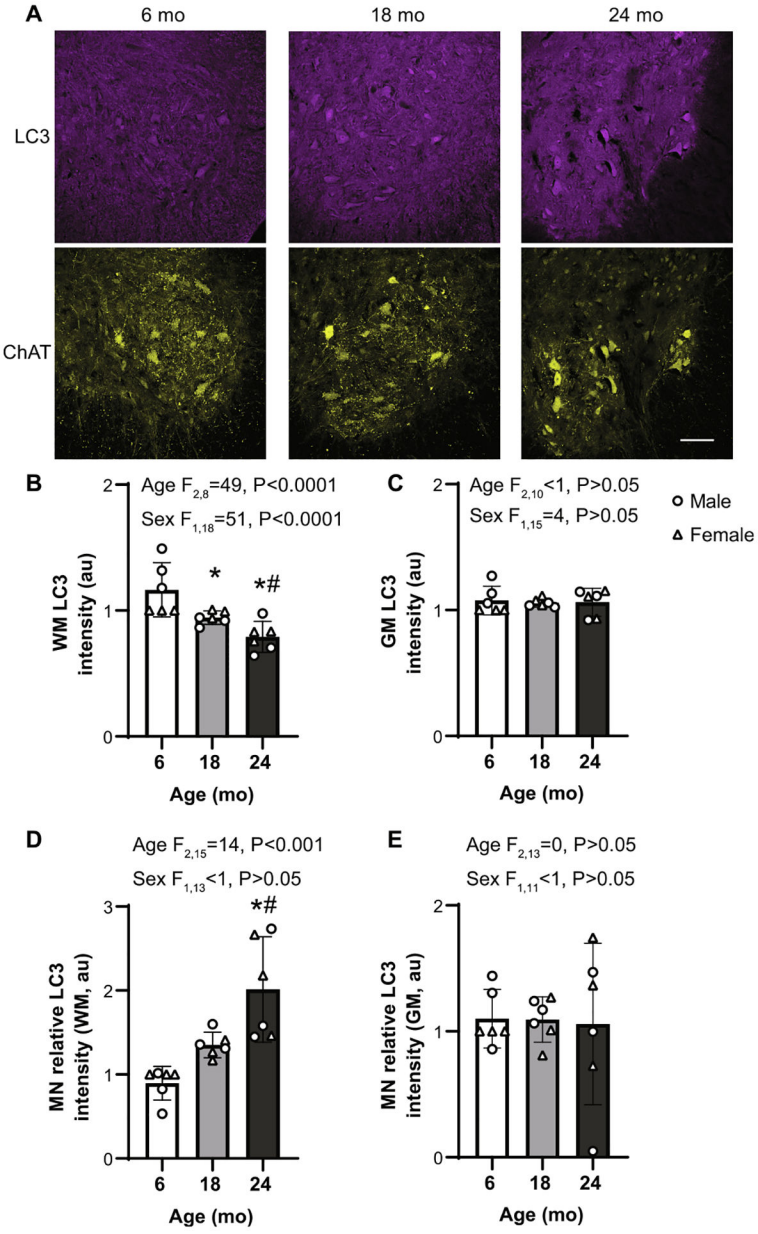

Fig. 3.

A) Representative images of LC3 and ChAT immunofluorescence in 6, 18, and 24 month old (mo) mice. Maximum intensity projection images for LC3 (magenta, upper panels) and motor neurons (ChAT+, yellow, lower panels). Immunofluorescence intensity was measured for LC3 in ChAT-positive motor neurons, gray and white matter (GM and WM, respectively) as in Fig. 2. (B–E) Bar graphs show mean ± 95 % CI of individual measurements of LC3 expression averaged per animal and normalized to the 6 mo female for each slide for B) WM, C) GM, D) MNs relative to the WM, and E) MNs relative to the GM. Intensity units are arbitrary (au). WM LC3 intensity decreased at 18 and 24 mo compared to 6 mo mice, and further decreased at 24 mo compared to 18 mo. This is while GM and MN LC3 relative to GM remained unchanged. LC3 expression in MNs relative to WM increased significantly

at 24 mo compared to 6 and 18 mo. Statistics shown are from mixed linear model of individual MN measurements with age, sex, and their interactions as fixed effects and animal as random effect. *, significantly different than 6 mo. #, significantly different than 18 mo. Bar, 100 μm.

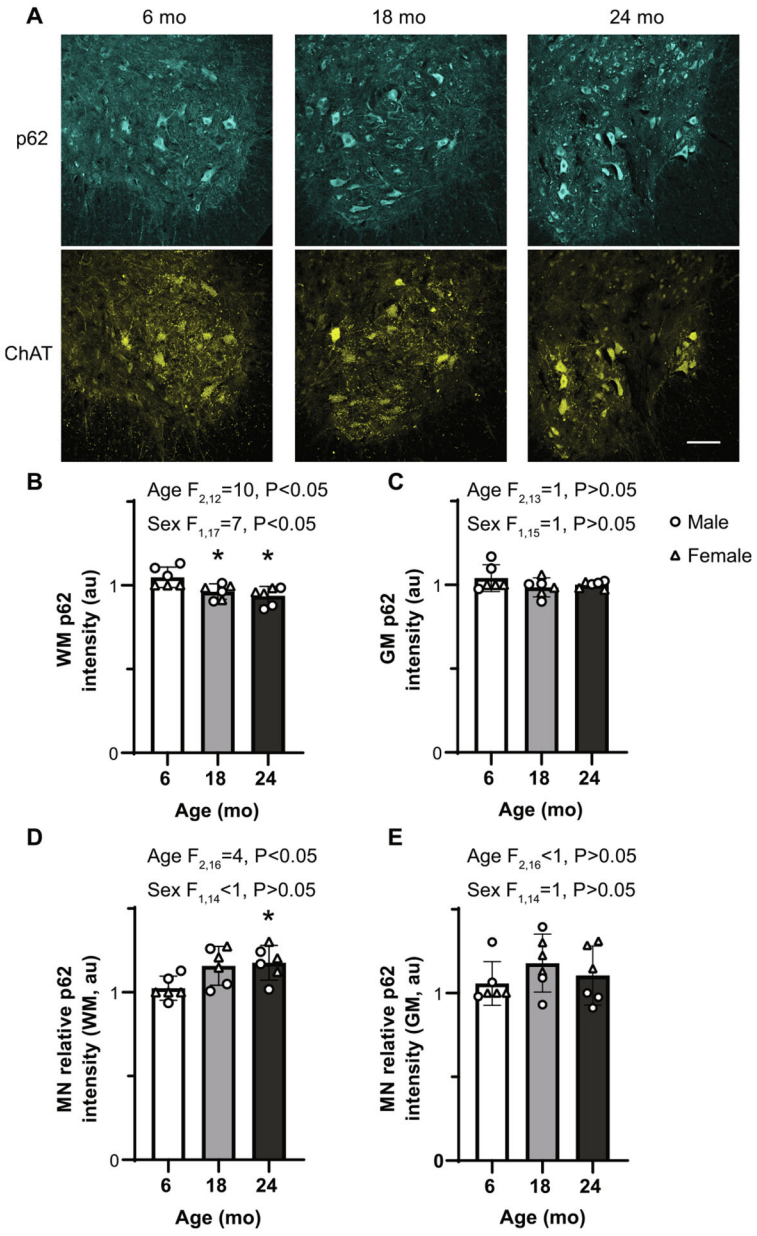

Fig. 4.

A) Representative image of p62 and ChAT immunofluorescence in 6, 18, and 24 month old (mo) mice. Maximum intensity projection images for p62 (cyan, upper panels) and motor neurons (ChAT+, yellow, lower panels). Immunofluorescence intensity was measured for p62 in ChAT-positive motor neurons, gray and white matter (GM and WM, respectively) as in Fig. 2. (B–E) Bar graphs show mean ± 95 % CI of individual measurements of p62 expression per animal normalized to the 6 mo female for each slide for B) WM, C) GM, D) MNs relative to the WM and E) MNs relative to the GM. WM p62 intensity decreased at 18 and 24 mo compared to 6 mo mice. This is while GM and MN p62 relative to GM remained unchanged. p62 expression in MNs relative to WM increased significantly at 24 mo compared to 6 mo. Intensity units are arbitrary (au). Statistics shown are from mixed

linear model of individual MN measurements with age, sex, and their interactions as fixed effects and animal as random effect. *, significantly different than 6 mo. #, significantly different than 18 mo. Bar, 100 μm.

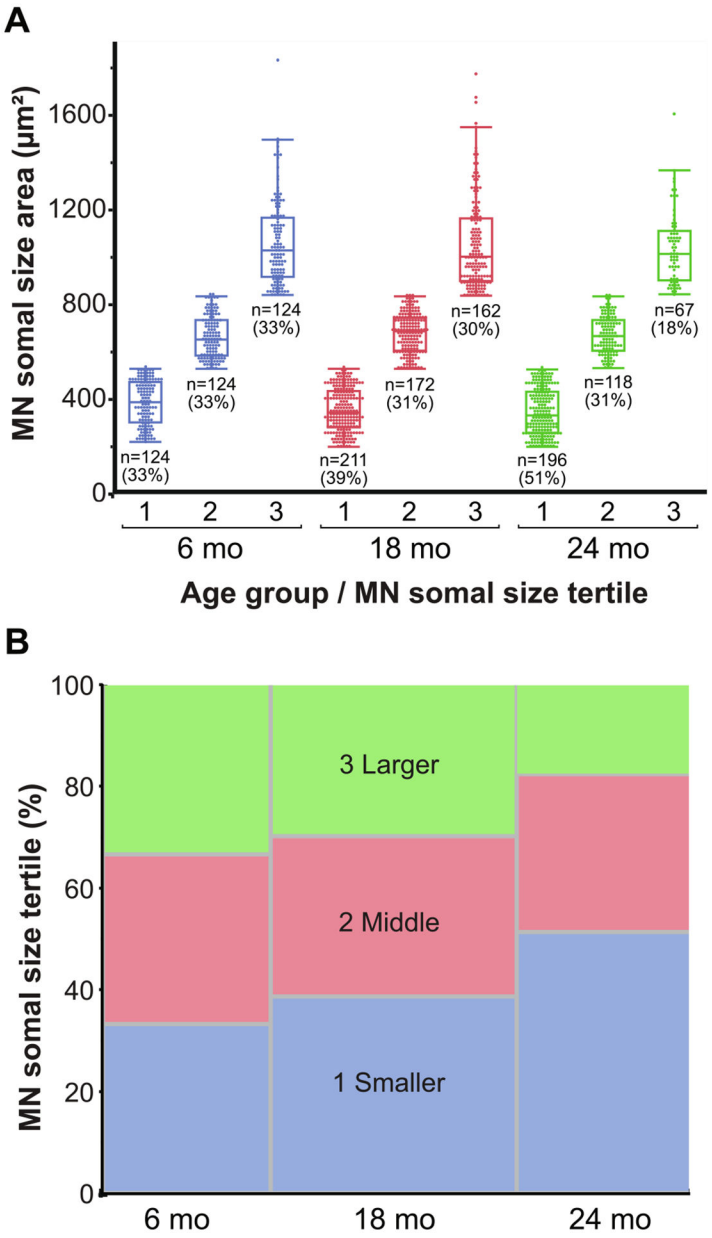

Fig. 5.

A) Distribution of MN somal size across age groups. MNs were classified into tertiles by somal cross-sectional area in the 6 mo group, and these criteria were applied to the older 18 and 24 mo groups and tertiles. The numbers of MNs in each tertile and age group are included below each box plot. B) Mosaic plot shows MN somal size tertiles in different age groups. Wider mosaic area in the 18 mo age group indicates greater number of MNs were present in this group. The number of MNs in the larger tertiles decreases with age, Chi-square $p < 0.0001$.

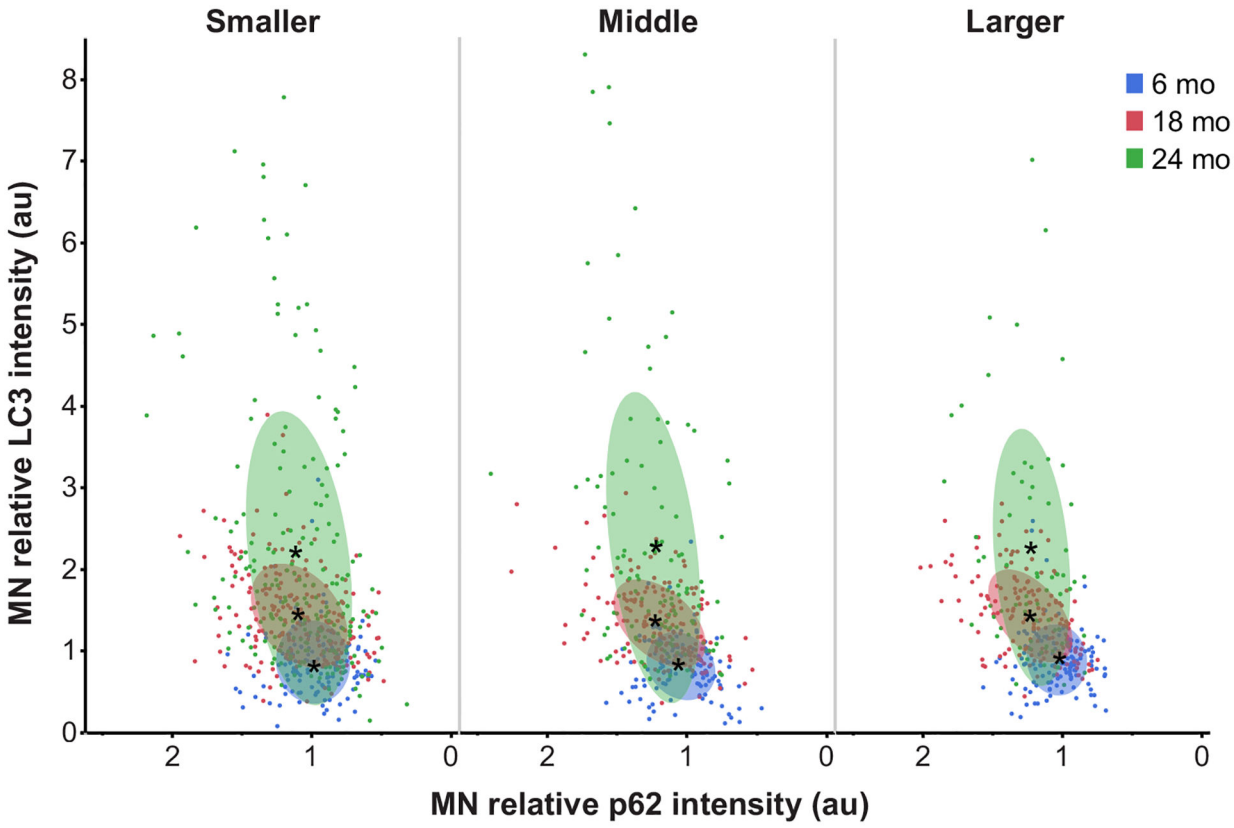

Fig. 6.

Correlation between LC3B and p62 relative fluorescence intensity in individual motor neurons in the lumbar spinal cord of mice shown in different groups based on motor neuron soma size tertiles. Each point represents an individual motor neuron and colors represent age groups. Shaded areas show bivariate normal density ellipses (50 % of distribution) for each age group. Across all tertiles, there was an upward and leftward shift with aging, reflecting the age-related increase in relative LC3 and p62 expression. This shift is consistent across all MN somal size tertiles. *, shows the center of each ellipse.

Table 1

Number of motor neurons [N (%)] in each age and sex group according to spinal cord level.

		Age group					
		6-Month		18-Month		24-Month	
	Sex	F	M	F	M	F	M
Spinal level	L1	0 (0 %)	0 (0 %)	10 (5 %)	0 (0 %)	18 (8 %)	43 (28 %)
	L2	35 (15 %)	0 (0 %)	58 (31 %)	93 (26 %)	27 (12 %)	47 (31 %)
	L3	89 (38 %)	34 (25 %)	48 (25 %)	161 (45 %)	126 (55 %)	51 (34 %)
	L4	50 (21 %)	6 (4 %)	13 (7 %)	24 (7 %)	13 (6 %)	11 (7 %)
	L5	43 (18 %)	92 (67 %)	60 (32 %)	78 (22 %)	45 (20 %)	0 (0 %)
	L6	18 (8 %)	5 (4 %)	0 (0 %)	0 (0 %)	0 (0 %)	0 (0 %)
	Total #MNs	235	137	189	356	229	152

F = Female, M = Male.

Table 2

Distribution of motor neurons [N (%)] in each age and sex group according to MN pool.

		Age group					
		6-Month		18-Month		24-Month	
	Sex	F	M	F	M	F	M
MN pool	Quadratus lumborum (L1)	20 (9 %)	0 (0 %)	2 (1 %)	28 (8 %)	14 (6 %)	34 (22 %)
	Axial (L1-L5)	36 (15 %)	10 (7 %)	31 (16 %)	43 (12 %)	17 (7 %)	19 (13 %)
	Quadriceps (L2-L3)	74 (31 %)	29 (21 %)	93 (49 %)	184 (52 %)	140 (61 %)	88 (58 %)
	Crural extensors (L4-L5)	19 (8 %)	19 (14 %)	20 (11 %)	29 (8 %)	13 (6 %)	2 (1 %)
	Crural flexors (L4-L5)	24 (10 %)	24 (18 %)	13 (7 %)	31 (9 %)	19 (8 %)	4 (3 %)
	Hamstring (L4-L6)	62 (26 %)	55 (40 %)	30 (16 %)	41 (12 %)	26 (11 %)	5 (3 %)
	Total #MNs	235	137	189	356	229	152

MN = Motor neuron.